Seismic vulnerability and loss assessment of Vila Real de Santo António, Portugal: application of a novel method

Javier Ortega[a*], Graça Vasconcelos[a], Hugo Rodrigues[b], Mariana Correia[c]

[a] ISISE, Department of Civil Engineering, University of Minho, Guimarães, Campus de Azurém, 4800-058 Guimarães, Portugal; javier.ortega@civil.uminho.pt (J. Ortega); graca@civil.uminho.pt (G. Vasconcelos)

[b] RISCO, School of Technology and Management, Polytechnic Institute of Leiria, Campus 2, 2411-901 Leiria, Portugal; e.mail: hugo.f.rodrigues@ipleiria.pt (H. Rodrigues)

[c] CI-ESG Research Centre, Escola Superior Gallaecia, Vila Nova de Cerveira, Portugal; e.mail: marianacorreia@esg.pt (M. Correia)

* Corresponding author; e-mail: javier.ortega@civil.uminho.pt

Abstract: The city of Vila Real de Santo António (VRSA) was erected after the 1755 Lisbon earthquake following a *Pombaline* development similar to the well-known reconstruction of Lisbon downtown. It included seismic resistant measures at an urban and architectural level, but most original buildings have nowadays been replaced or are highly altered. A research question arises whether or not and to what extent these alterations have compromised the seismic vulnerability of the historical city center. The paper presents the seismic vulnerability assessment of the historic city center of VRSA using a newly developed method: Seismic Assessment of the Vulnerability of Vernacular Architecture Structures (SAVVAS). The method proposes a numerical tool intended to estimate the seismic capacity of vernacular buildings using qualitative and simple quantitative data that can be rapidly obtained from visual inspections. The seismic vulnerability and loss assessment considers different scenarios, including the historical condition, and studies different retrofitting strategies.

Keywords: Seismic vulnerability assessment; Vernacular architecture; Damage scenarios; Historical city center; Loss estimation; Urban retrofitting strategies

1. Introduction

Vila Real de Santo Antonio (VRSA) is located in Algarve, the southernmost area of Portugal. This region was considerably affected by the 1755 Lisbon earthquake and was practically abandoned at the time. As an attempt to boost the Algarve local economy through industrial development, the Marquis of Pombal enacted an official recovery program during the 1760s and 1770s that included the construction from scratch of the city of VRSA. The strategic position of this new city, at the South coast of the Algarve, facing the Spanish border, was also intended to control port transactions and was a display of political power (Correia 1997). Since VRSA is contemporary to the reconstruction of Lisbon downtown, they share many similarities and are based on the same ideas and criteria, resulting in a similar urban and architectural design in terms of composition and rigorous geometric clarity, as well as in the social and industrial functionality.

As a reaction to the devastating 1755 earthquake, both the buildings and the urban plan were earthquake-inspired and designed to protect people in a seismic event. The *Pombaline* city plan consists of a rectangular grid with one of the long sides placed along the Guadiana River, facing east (Figure 1). It is organized around a big central square and the streets were planned sufficiently wide to allow a proper evacuation in the event of an earthquake. Most of the buildings belonged to four distinct architectural building types defining a clear hierarchy at an urban level (Figure 1). Their structural system mainly consisted of load bearing stone masonry walls as the main vertical resisting elements, coupled with horizontal timber diaphragms (floors and roofs). The most notable seismic resistant constructive solution, applied only at the buildings with more than one floor (riverfront buildings and square buildings from Figure 1), was the inclusion of timber frame partition *frontal* walls connecting the timber roof and the timber floor structures, analogous to the system developed for the reconstruction of Lisbon and known as *gaiola Pombalina*. In addition, some ground floor rooms had vaulted ceilings supporting the first floor as a fire prevention measure, as occurred in Lisbon (Mascarenhas 1996). The seismic concern that emerged after the earthquake can also be perceived in the generalized good quality and strength of the original buildings of VRSA (Oliveira 2009).

Nowadays, the great majority of the original buildings have been replaced by new ones or are highly altered at a formal and structural level. There has been a transformation process in the city mainly characterized by a massive unplanned occupation of the blocks' patios with additional constructions, leading to a densification of the urban fabric. The single-story dwellings were the main target of the demolitions, substitutions and large modifications. The most common modifications consisted of the addition of new floors, the enlargement or addition of new openings or the substitution of the timber floors and roofs. This transformation process is a distinct characteristic of vernacular architecture in urban environments, which has an open-ended and spontaneous nature because of changes in the use of the buildings due to the new needs of the users. However, the deep mischaracterization of the built-up environment is not only detrimental in terms of loss of authenticity of an important architectural and urban heritage, but also reflects the loss of seismic awareness, as the initially adopted effective seismic resistant measures, including the characteristic *Pombaline* timber frame partition *frontal* walls, have been abandoned and the careful architectural design has been neglected.

Figure 1. Original plan of VRSA city center and main building types (adapted from Rossa 2009)

The present work presents the seismic vulnerability assessment of VRSA historical city center carried out using the recently developed Seismic Assessment of the Vulnerability of Vernacular Architecture Structures (SAVVAS) method (Ortega et al. 2019a). Seismic vulnerability assessment methods are valuable tools intended to evaluate the seismic risk of buildings by providing an estimation the damage that a certain structure will suffer after a seismic event of a given intensity. Among the many methods available in the literature, large scale analyses comprising a large number of buildings require simplified (first level) approaches that rely on less detailed qualitative information related to a few parameters that can be obtained with simple expedited visual inspections.

This type of simplified seismic vulnerability assessment approaches are typically empirical methods, based on knowledge acquired through post-earthquake damage observation and expert judgment. The SAVVAS method is also conceived as a first level approach, but has been developed using an analytical procedure instead of an empirical one. It mainly consists of a numerical tool intended to estimate the seismic capacity of vernacular unreinforced masonry and earthen buildings using qualitative and simple quantitative data. It should be noted that the SAVVAS method is here applied for the first time in a case study and the present paper thus shows its capabilities and potential as a first level seismic vulnerability assessment method.

In addition to discussing the seismic vulnerability of the current condition of VRSA city center, two additional scenarios are evaluated. First, the historical configuration of the city center was studied and its seismic vulnerability is evaluated. This intends to understand if the deep alteration of the city at an urban and building level has compromised the seismic vulnerability of the historical city center and to what extent, which is one of the main research questions investigated in the present study. Secondly, the paper analyzes how to apply the SAVVAS method as a tool for managing seismic risk of historic urban areas. Different possible retrofitting strategies, based on traditional earthquake resistant solutions, were considered at an urban level and their efficiency in reducing the seismic vulnerability of VRSA city center was evaluated. The study ends with the seismic loss assessment of VRSA, in terms of collapsed and unusable buildings, number of casualties and homelessness, and repair costs. This loss estimation is also carried out for the different abovementioned scenarios, allowing the comparison among the results obtained.

2. The SAVVAS method

The SAVVAS method used to carry out the seismic vulnerability assessment of VRSA is intended to be an expedited simplified approach that provides the possibility of performing a primary seismic safety assessment of a vernacular building or group of buildings based on simple surveys that can be carried out even solely by means of visual inspection. It was developed using an analytical process that included an extensive numerical parametric study based on detailed finite element modeling and nonlinear analysis. The thorough numerical campaign was intended to quantify the influence of a set of geometrical, structural, constructive and material parameters in the seismic response of vernacular buildings. The results of the parametric analysis were assembled into an extensive database that was later used to develop regression models using data mining techniques. As a result, the SAVVAS method proposes a numerical tool consisting of different formulations that allow defining the seismic capacity of the building in quantitative terms, through seismic load factors expressed as accelerations (in terms of *g*) associated with different structural damage limit states (LS). The input of these formulations are simple variables based on the ten key seismic vulnerability assessment parameters selected (Figure 2). The reader is referred to Ortega (2018) for an in-depth explanation of the development of the SAVVAS method.

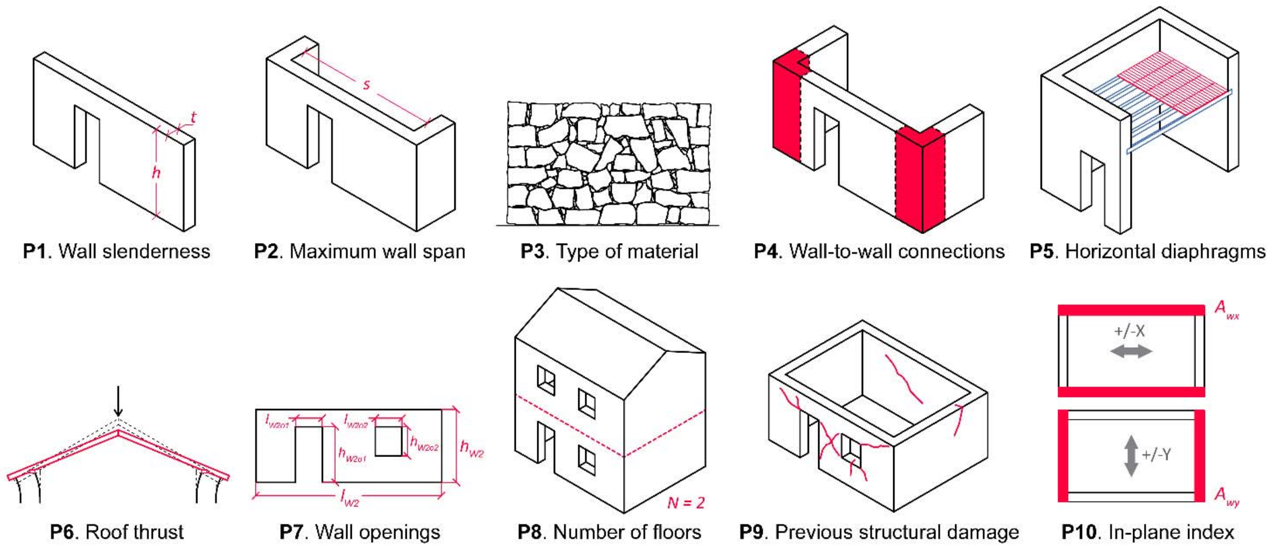

Figure 2. Seismic vulnerability assessment parameters of the SAVVAS method

The ten parameters were selected based on seismic vulnerability methods existing in the literature, namely vulnerability index approaches, which also measure the seismic vulnerability of a building as a function of a set of parameters (Benedetti and Petrini 1984; Boukri and Bensaibi 2008; Vicente et al. 2011, Ferreira et al. 2014; Shakya 2014). Also following the vulnerability index approach, four classes of increasing seismic vulnerability were defined for each parameter, from 1 (lowest) to 4 (highest), based on the previously mentioned extensive numerical parametric campaign (Ortega et al. 2019a). The SAVVAS formulation and procedure is shown in Table 1. The first step of the SAVVAS method is precisely the assignment of seismic vulnerability classes to some of the parameters (P3, P4, P5, P6 and P9). However, as shown in Table 1, while these five parameters are defined in qualitative terms, as a function of their class, the remaining ones are defined through specific quantitative attributes. As an example, P2 (maximum wall span) is directly defined by the span (in *m*). The same occurs for P1, P7, P8 and P10. It should be noted that parameter P7 (wall openings) is divided into two parameters because it distinguishes between the role of wall openings when the wall is subjected to out-of-plane loading and when is subjected to in-plane loading.

Table 1. SAVVAS formulation and procedure

Step 1	**Definition of the seismic vulnerability assessment parameters**		
	P1	λ	Ratio between the effective wall inter-story height (*h*) and its thickness (*t*)
	P2	s	Maximum wall span without intermediate supports measured in meters (*m*)
	P3	*[1-4]*	Seismic vulnerability class of the building according to P3 (type of material)
	P4	*[1-4]*	Seismic vulnerability class of the building according to P4 (wall-to-wall connections)
	P5	*[1-4]*	Seismic vulnerability class of the building according to P5 (horizontal diaphragms)
	P6	*[1-4]*	Seismic vulnerability class of the building according to P6 (roof thrust)
	P7	$P7a$	Ratio between the area of wall openings in a wall perpendicular to the loading direction and the total area of openings in the considered wall
		$P7b$	Ratio between the area of wall openings in all in-plane resisting walls and the total area of all in-plane resisting walls
	P8	N	Number of floors
	P9	*[1-4]*	Seismic vulnerability class of the building according to P9 (previous structural damage)
	P10	γ_i	Ratio between the in-plan area of earthquake resistant walls in the loading direction and the total in-plan area of earthquake resistant walls
Step 2	**Calculation of the load factors associated to the limit states in each main direction i (in terms of g)**		
	$LS1_i = e^{(1.97-0.06\lambda-0.1s-0.68\ln(P3)-0.14P4-0.28P5-0.39\ln(P6)-3.43P7b-0.82\ln(N)-2.27\ln(P9)+0.63P5P7b)} - c$		
	$LS2_i = 0.16 \times LS1(g) + 0.78 \times LS3(g)$		
	$LS3_i = e^{(2.16-0.04\lambda-0.05s-0.24P3-0.16P4-0.28P5-0.08P6+0.3P7a-2.79P7b-0.37N-0.15P9+0.74\gamma_i+0.44P5P7b)}$		
Step 3	**Calculation of the global load factors defining the limit states of the building (in terms of g)**		
	$LS1 = \min(LS1_i)$		
	$LS2 = \min(LS2_i)$		
	$LS3 = \min(LS3_i)$		

With respect to the structural limit states (LS1, LS2 and LS3), they are associated to specific damage levels exhibited by the structure, defined according the force-displacement pushover curve resulting from the nonlinear numerical parametric study (Figure 3). LS1 can be associated to the formation of the first cracks in the structure. Before this limit, the structural behavior of the building remains in the elastic part and the structure can be considered as fully operational. LS2 depicts the transition between a point where the structure is still functional, retaining most of its original stiffness and strength, showing minor structural damage, and a state where significant damage is visible so that the building could not be used after without significant repair. LS3 is defined by the load factor and displacement corresponding to the attainment of the building maximum resistance. As a result, the building has lost a significant amount of its original stiffness, but is supposed to retain some lateral strength and margin against collapse even if it cannot be used after the earthquake. It is noted that the fourth limit state (LS4) was excluded because it corresponds to the point where the building maximum strength is reduced 20%, thus being mathematically dependent on LS3. The load factor associated to the collapse of the building is thus not defined according to this pushover curve, but was calibrated in a subsequent step using post-earthquake damage data (Ortega et al. 2019b).

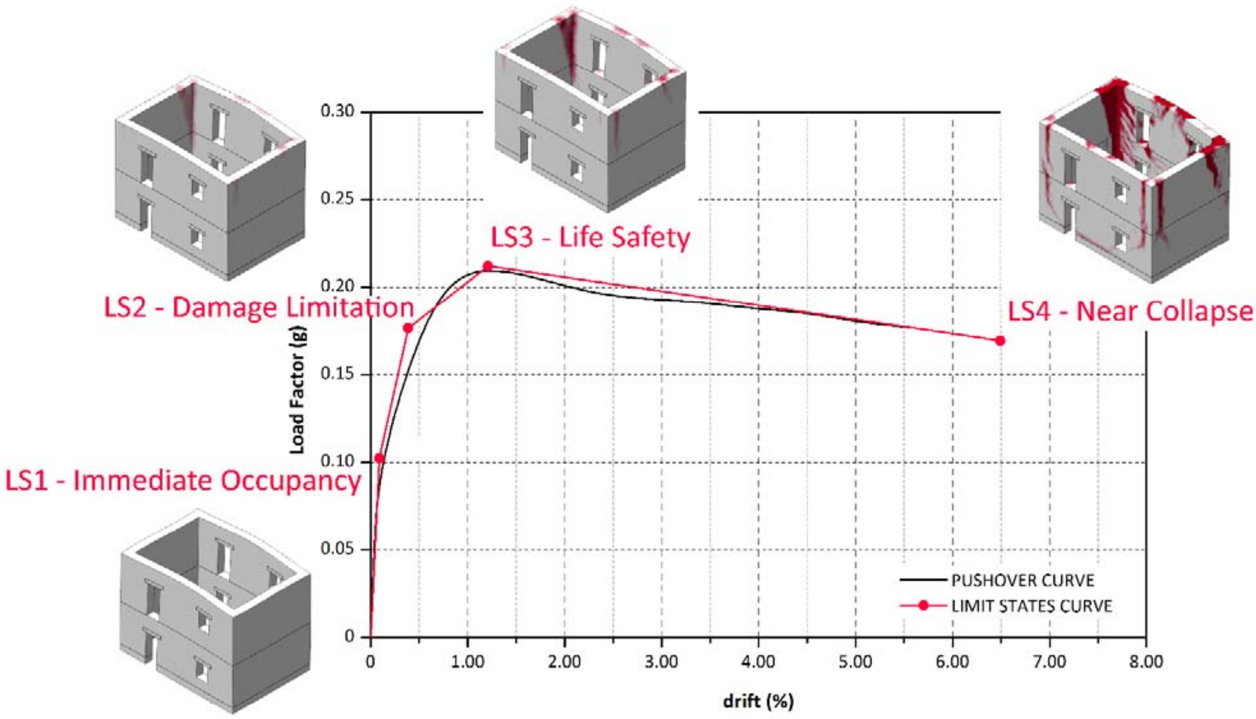

Figure 3. Definition of the limit states according to the pushover curve (Ortega et al. 2019a)

The load factors calculated with the SAVVAS formulation can be associated to the seismic actions that can cause the building to reach the different structural limit states. They can be calculated for the four main directions of the building (+/-X and +/-Y), which allows an estimation of its most vulnerable direction. Nevertheless, in order to provide a global seismic assessment of the building, the minimum values for each LS among the four resisting directions are given as global load factors defining its seismic vulnerability. This is the last and third step of the procedure and, as a result, the SAVVAS method provides an estimation of the minimum load that will cause the building to reach the different limit states.

3. Building characterization

The transformation process that took place in the 1773 *Pombaline* core of VRSA motivated important research work promoted by the city hall (SGU 2008). The work consisted of an analysis carried out on a building-by-building basis intended to identify the remaining original *Pombaline* buildings and their morphological relationship with respect to the original design. According to Gonçalves (2005), results indicated that only 5% of the buildings still preserve unaltered original characteristics in terms of elevation and 8% in terms of volume. The survey showed that even though stone masonry still is the construction system of the majority of the buildings, less than 20% of the buildings are the original *Pombaline* buildings constructed in the 18th century. Around 54% of the built-up fabric was constructed during the 20th century. The numbers clearly illustrate the significant alterations done in the historical city center and the degradation of the ideal originally designed plan. Figure 4 shows examples of the deep alterations on the built-up environment that took place in the last century in VRSA and a comparison between the original and the current urban plan.

(a) (b) (c) (d)

Figure 4. (a-c) Typical alterations occurred throughout the 20th century: original versus current condition (adapted from Gonçalves 2009); and (d) comparison between the original and current plan of VRSA city center

The data collected by SGU (2008) allowed identifying those buildings in the city center whose main construction system still consisted on stone masonry walls and timber floor and roof structures. From a total of 490 buildings located *Pombaline* core of VRSA, 284 stone masonry buildings were selected to perform the seismic vulnerability assessment. The remaining buildings either present R/C structures or mixed construction systems made them not applicable for the SAVVAS method. Among these 284 buildings, 7 buildings were identified as original unaltered buildings and 77 were constructed in the 18th century, but show significant structural alterations. The remaining 200 buildings are substitutions of the original buildings and were constructed during the 19^{th} and 20^{th} century. Figure 5 shows examples of the three types of buildings that were evaluated, classified according to their date of construction and altered condition. Figure 6 summarizes this data and shows the urban plan, identifying the buildings that were selected for the seismic vulnerability assessment.

The data available included urban plans and detailed reports on the construction characteristics and state of conservation of most of the buildings, including interior and exterior photographs. Additionally, a field visit was carried out, which allowed gathering more information from these buildings. Most of the buildings could only be inspected from the exterior, but some specific buildings could be surveyed more in detail, obtaining information of the different structural elements (roof, floors, masonry walls, partition walls, etc.). As an example, the *Alfândega* or Customs House was thoroughly studied through historical survey, visual inspection and experimental in-situ dynamic identification, which allowed calibrating numerical models and estimate material properties (Ortega et al. 2016). Since VRSA was constructed simultaneously, a great homogeneity in the building characteristics was generally observed. Thus, the data gathered from the buildings that were inspected in detail could be extrapolated to those buildings for which less information was available.

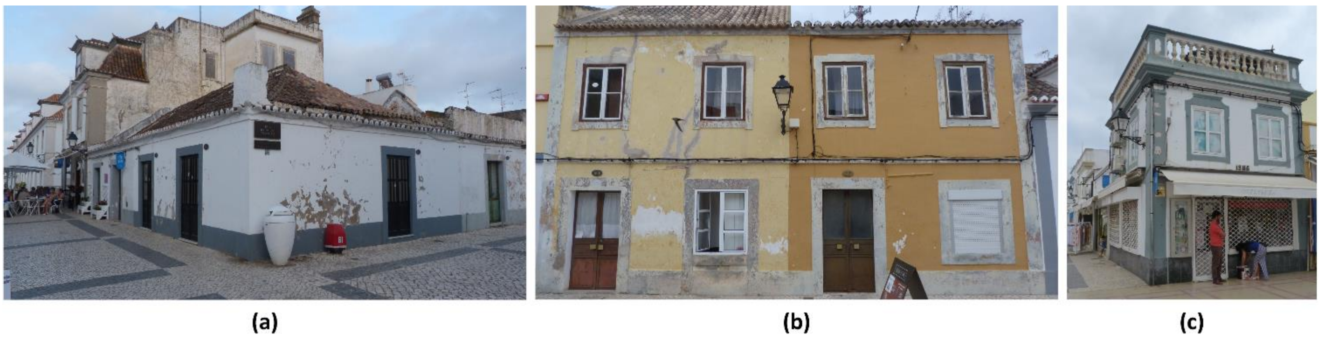

Figure 5. Examples of typical traditional stone masonry buildings in VRSA selected for the seismic vulnerability assessment: (a) original unaltered building; (b) original building with alterations (addition of new floors); and (c) non-original building constructed in the 19th century

Figure 6. Evaluated buildings in VRSA city center classified according to their date of construction and altered condition

4. Seismic vulnerability assessment

The information collected for the building characterization allowed performing the seismic vulnerability assessment of VRSA city center. The results obtained from the assessment are discussed also aiming at extracting conclusions on the applicability of the SAVVAS method. In a second step, since the information collected included a wide set of data on the historical condition of the city, including detailed plans and construction details of the original buildings, the seismic vulnerability assessment of the historical configuration of VRSA city center could be performed. The paper shows a comparative analysis between the historical and current condition in terms of seismic vulnerability. Finally, this section presents and discusses several retrofitting strategies based on traditional solutions and evaluates their efficiency in reducing the seismic vulnerability of VRSA.

4.1. Seismic demand

Since the load factors that define each LS are expressed in terms of g, they can be compared with an expected seismic event expressed in terms of accelerations. The Italian code (MIT 2018) provides recommendations on the way to consider the spectral seismic demand (S_e) for a given peak ground acceleration (PGA) in a simplified way, which can be later compared with the acceleration capacity of the structure, given by the different LS previously determined. The method, termed as linear by the code, specifies that the seismic demand (S_e) can be computed according to the spectrum using Eq. 1.

$$S_e(T_B \leq T \leq T_C) = a_g \cdot S \cdot \eta \cdot F_0 \tag{1}$$

where a_g is the value of the PGA (in g), S is a coefficient related with the soil conditions, η is the damping correction factor and F_0 is a coefficient that quantifies the maximum spectral amplification, on a horizontal rigid reference site, and has a minimum value of 2.2. It should be noted that the seismic demand calculated according to the response spectrum depends on the natural period of vibration of the building. In this case, a natural period within the interval between T_B and T_C is assumed, which lies in a value within the plateau of the spectrum and results in the maximum possible demand. Thus, while simplifying the calculation, the values obtained are conservative, which is in agreement with the simplified philosophy of the SAVVAS method. The Italian code also states that the dissipative capacity of the structure can be considered through the reduction of the demand, taking into account in a simplified way the inelastic behavior of the structure, its overstress and the increase of its own vibration period following plasticization. To assess the demand, the value obtained from the spectrum can be reduced by substituting η with $1/q$ in Eq. 1, where q is the behavior factor of the structure and can be computed using Eq. 2.

$$q = q_0 \cdot K_R \tag{2}$$

Where q_0 is obtained from the code and for unreinforced masonry results in a value of 2.98, and K_R is a factor that depends on the regularity in height of the structure, taking values of 1 for regular and 0.8 for irregular structures. Assuming a common irregularity of the structures, considering a soil type C (medium quality), in the absence of specific data, and no topographic amplification, the correlation between the PGA (a_g) and the seismic demand (S_e) is shown in Eq. 3.

$$S_e = a_g \cdot 1.4 \tag{3}$$

It should be highlighted that this is a preliminary seismic vulnerability assessment that can be carried out in an expedited way comparing the results obtained after applying the SAVVAS method directly with the seismic demand established by the codes (NP EN1998-1 2010; MIT 2018). As previously stated, the SAVVAS method was conceived as a tool that allows to estimate the acceleration capacity of the structure using qualitative and simple quantitative data, that can be easily obtained from visual inspections. More refined and sophisticated assessments, such as the well-established N2 method proposed by the Eurocode 8 (CEN 2004) or the nonlinear static analysis established by the Italian code (MIT 2018), are beyond the scope of the method. This is nonetheless, an open future path of investigation to refine the method.

4.2. Current condition

The SAVVAS method was applied on the 284 existing masonry buildings. After performing the building on-site characterization, which allows assigning values for all parameters for each building, the expressions shown in Table 1 (step 2 and 3) could be used. As a result, the minimum load factors associated to the three main limit states (LS1, LS2 and LS3) were calculated for each building. Subsequently, the mean values of the load factors for the whole city center could be computed, which are 0.15g, 0.35g and 0.42g for LS1, LS2 and LS3 respectively. It should be noted that these values show high variability with a STD (σ_{LS}) of 0.14g, 0.13g and 0.14g, which result in CoV of 93%, 36% and 33%.

Therefore, in order to have a primary idea of the vulnerability of the building stock, the values obtained can be compared with the seismic demand, estimated from the PGA defined by the code. For Vila Real de Santo António, the value of PGA reference value is 0.17g (NP EN1998-1 2010), which, according to Eq. 3, results in a value of seismic demand $S_e = 0.24g$. It should be noted that, since the present simplified assessment does not take into consideration the fundamental period of the building, the highest value of PGA between the two established for Type 1 and Type 2 seismic actions was considered. A total of 27 buildings, representing approximately 10% of the buildings analyzed, present a load factor defining LS3 below 0.24g, i.e. their maximum capacity is likely to be exceeded for an earthquake of the characteristics defined by the code. This fact shows a non-negligible risk that should be taken into consideration for future urban retrofitting strategies of the building stock. Moreover, most of the buildings are prone to suffer slight structural damage, since the load factor defining LS1 for over 70% of the buildings evaluated is below this limit of 0.24g. The great amount of buildings obtained with a very low load factor defining LS1 is mostly due to the poor state of conservation of many buildings, which already show slight structural damage.

To obtain a better understanding of the characteristics of the buildings evaluated, Table 2 shows the statistics from the values defining each parameter and the computed global load factors defining the three limit states. Given the low variations for parameters P1, P3 and P5, the table confirms that the main building structural typology evaluated is similar, consisting of thick load bearing irregular masonry walls (class 3 for P3) coupled with flexible timber horizontal diaphragms (class 4 for P5). It should be noted that the class for the masonry was assigned based on the previously mentioned experimental investigation (Ortega et al. 2016), which was performed on a building that presents the original walls. Thus, the type of material used for buildings constructed at a later stage (19th or 20th century) might not be the same. However, the same class was assumed for all buildings in the absence of more detailed information. The same criterion applies to other constructive parameters such as P1 and P5. Proper connection among orthogonal walls was considered for most of the buildings (class 2 for P4), since they were originally workmanlike constructed. Class 1 was considered for those buildings with a greater symbolic value, such as the riverfront buildings due to the presence of quoins. The roof type (P6) was quite variable, being one of the structural elements that suffered more alterations.

Table 2. Statistics from the parametric survey and the estimated load factors defining each limit state

Variables		**Units**	**Minimum**	**Maximum**	**Mean**	**Median**	**Mode**	**STD**	**CoV**
Parameters	**P1**	λ	4.55	6.82	5.15	5.30	5.30	0.50	9.71%
	P2	*m*	2.25	21.2	6.78	5.50	4.50	3.17	46.67%
	P3	Class	2	3	2.99	3	3	0.08	2.79%
	P4	Class	1	3	1.90	2	2	0.32	16.97%
	P5	Class	3	4	3.88	4	4	0.32	8.27%
	P6	Class	1	3	1.83	2	1	0.89	48.54%
	P7a	*P7a*	0	0.51	0.18	0.20	0	0.09	53.14%
	P7b	*P7b*	0	0.57	0.05	0.03	0	0.07	123.60%
	P8	*N*	1	3	1.37	1	1	0.50	36.47%
	P9	Class	1	3	1.59	1	0.66	0.66	41.28%
	P10	γ_i	0.28	0.69	0.48	0.50	0.50	0.05	9.81%
Load factor	**LS1**	*g*	0.00	0.50	0.15	0.09	0.03	0.14	93.21%
	LS2	*g*	0.10	0.69	0.35	0.34	0.27	0.13	35.88%
	LS3	*g*	0.13	0.79	0.42	0.40	0.33	0.14	33.03%

In terms of geometry, the buildings are typically very regular with an almost square configuration ($\gamma_i \cong 0.5$) and a very low CoV. However, the extremely regular subdivision observed in the historical configuration has been lost. Many party walls have been demolished in order to join several buildings, and new buildings were constructed in the place previously occupied by two or more buildings. As a result, some of the façade walls present large spans and, consequently parameter P2 shows a high variability. It is noted that the interior condition of these buildings could not be inspected in many cases and had to be assumed from the exterior. Nonetheless, the general low values for P2 and P8 confirm that the VRSA city center mainly comprises one-floor buildings of reduced scale. Buildings with two and three floors typically show a high amount of wall openings, in contrast with the few openings of single-story buildings, reflecting high values of CoV for parameters P7a and P7b. Results also show a high variability regarding P9 (previous structural damage). There are several buildings that were considered as Class 2 and 3 for P9, due to a clear lack of maintenance and abandonment. Some of the buildings inspected showed big structural cracks that, according to the reports from SGU (2008), were related with differential settlement.

Figure 7 shows the overall distribution of LS3 of the buildings within VRSA center. The distribution was mapped using ArcGIS Pro (Esri 2017), a GIS application that allows mapping the different damage and loss scenarios calculated from the seismic vulnerability assessment by associating information and structural characteristics to each building. These tools are very powerful for managing data, since they can be easily updated, and allows for a rapid visualization, selection and search of buildings within a given study area (Vicente et al. 2011). The resulting LS3 distribution map shown in Figure 7 can be particularly useful for the detection of the most vulnerable buildings that should be recommended for a more detailed inspection and assessment, in order to eventually decide on the need of retrofitting and how.

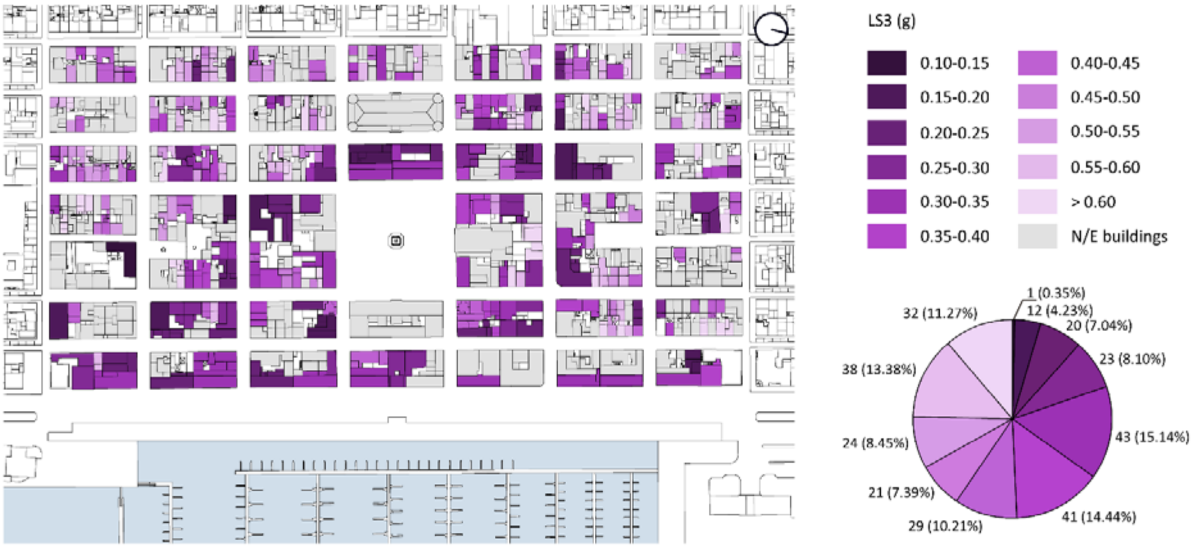

Figure 7. LS3 distribution in VRSA city center

4.2.1. Damage scenario

The next step of the application of the SAVVAS method is to correlate the three LS with damage grades. In this case, the damage grade classification used is based on the EMS-98 scale (Grünthal 1998), which is a widely used classification for first level seismic vulnerability assessments, such as the macroseismic method (Giovinazzi and Lagomarsino 2004). Thus, the output of the SAVVAS method can be comparable with them. Since the load factors related with the different structural damage LS are expressed as accelerations (in terms of g), they can be used in a straightforward way to eventually correlate the seismic demand (calculated from the PGA as shown in Eq. 1) with the expected damage. A correlation is thus established between seismic input (in terms of S_e), load factors associated to LS (expressed in g) and mean damage grade (μ_D) based on the EMS-98 scale, see Figure 8. It is noted that damage grade 0 was removed from the scale because the SAVVAS method does not detect non-structural damage (Ortega et al. 2019b). Grades 0 and 1 are thus the same and suppose the starting point of the scale. The load factor defining LS1 delimits the point where the building reaches damage grade 2 and starts presenting slight structural damage. Similarly, LS2 represents the threshold between damage grade 2 and 3, while LS3 is the threshold between damage grade 3 and 4. The load that would cause the total or near collapse of the building (damage grade 5) was defined by multiplying the value of LS3 with an empirically devised factor of 1.25, which was established and calibrated with post-earthquake damage data, see Ortega et al. (2019b). The damage values for the ranges of S_e between LS are obtained through simple linear interpolation, in order to provide a continuous variable.

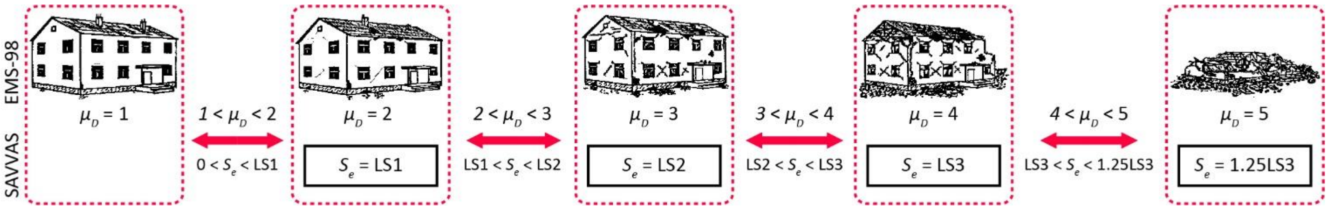

Figure 8. Correlation between the seismic input (**S_e**), SAVVAS limit states and EMS-98 damage grades

The GIS tool is also used to present the damage scenarios. Figure 9 shows the results for three different earthquake inputs: (a) $S_e = 0.15g$ $(PGA = 0.11g)$; (b) $S_e = 0.25g$ $(PGA = 0.18g)$; and (c) $S_e = 0.35g$ $(PGA = 0.25g)$. The maps show that few damage is expected for an earthquake with $S_e = 0.15g$, for which only a reduced number of buildings would reach a state of severe damage ($\mu_D > 3$) and only one shows values of damage close to potential collapse ($\mu_D > 4$). This is in agreement with the high values of LS3 obtained. As it could be expected, the risk highly increases for an earthquake scenario with $S_e = 0.35g$, for which the majority of the buildings are expected to either show a state of severe damage or be close to potential collapse. Nonetheless, there is a high variability and the SAVVAS method is able to individualize well the seismic behavior of each building and the maps show that there are several buildings presenting no structural damage even for an earthquake with $S_e = 0.35g$.

Figure 9. Damage scenarios for different seismic input in terms of **seismic demand (S_e)**: (a) 0.15g; (b) 0.25g; and (c) 0.35g

4.2.2. Fragility curves

As a final step, damage probability can be typically expressed using fragility curves. They define the probability ($P[D_k]$) of exceeding a fixed damage grade D_k ($k \in [1,5]$), defined by the different LS (Figure 8), as a function of the earthquake seismic demand (S_e) computed from the PGA (in terms of g). As recommended by other works dealing with the seismic vulnerability of historical structures (Saloustros et al. 2019), as well as available standards (FEMA 2010), the present works considers the lognormal cumulative distribution function to derive the analytical fragility curves. According to this distribution, the probability is calculated as a function of the mean and standard deviation of the natural logarithm of S_e at which the analyzed buildings reach the different LS. Figure 10a shows the fragility curves, which can be compared with the expected damage distribution obtained from the direct application of the method, see Figure 9. Curve D2 thus represents the percentage of buildings in VRSA that would probably exceed damage grade 2, which, for example, is 78%, for an earthquake with $S_e = 0.15g$. This is higher than the 57% predicted by the individual assessment shown in Figure 9a. However, the amount of buildings expected to exceed damage grade 3 according to the fragility function is 2%, which is more in agreement with the results shown in Figure 9c. Despite the differences obtained, it should be highlighted that, given the uncertainties associated with this type of simplified assessments (also related to the evaluation of the parameters), a statistical interpretation of the results is typically preferred (Ferreira et al. 2017).

Nevertheless, in order to further compare the results, another set of empirical fragility curves using the direct results of μ_D obtained for each building from the assessment, instead of a probability distribution function. Note that the values of the damage grades, $k \in [0,4]$, had to be used for mathematical purposes. Values 0 to 4 refers to the previously defined EMS-98 damage grades 1 to 5. The criterion adopted for belonging to each damage grade (D_k) is that $\mu_D \in [k - 0.5, k + 0.5]$. Thus, the probability p_k of belonging to each damage grade (μ_D) is:

$$p_k = \sum_{i=1}^{N} [k - 0.5 < \mu_{D_i} \leq k + 0.5] / N \tag{4}$$

where $[P] = 1$ if $[P]$ is true and $[P] = 0$ if $[P]$ is false, and N is the number of buildings evaluated. The fragility curves can be obtained by calculating the cumulative probability:

$$P[D_k] = \sum_{j=k}^{4} p_j \tag{5}$$

Figure 10b shows the fragility curves built using the expression shown in Eq. 5, as a function of the seismic input in terms of $\boldsymbol{S_e}$. These curves also show that for the previously mentioned earthquake defined by the code of $\boldsymbol{PGA = 0.17g\ (S_e = 0.24g)}$, approximately 10% of the buildings are expected to present severe damage with potential risk of collapse ($\mu_D > 4$). Slight structural damage is expected to occur even for earthquakes with low values of $\boldsymbol{S_e < 0.1g\ (PGA < 0.07g)}$, due to the poor state of conservation and previous structural damage observed in many buildings. These conclusions could be also detected from the damage scenarios shown in Figure 9.

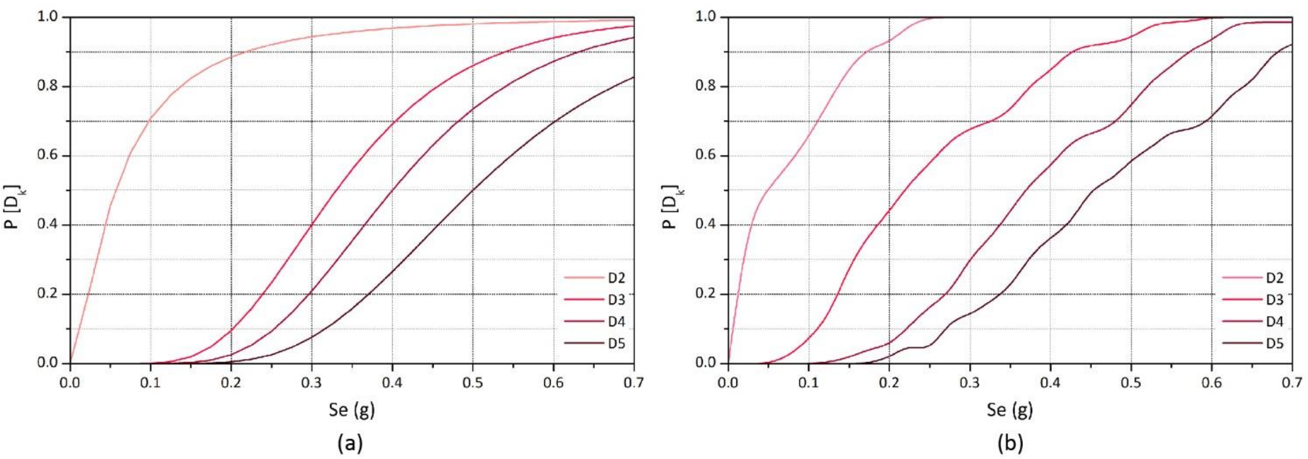

Figure 10. (a) analytical fragility curves adopting log-normal cumulative distribution function; and (b) empirical fragility curves

4.3. Historical vs current condition

As previously highlighted, VRSA was specifically conceived with high seismic awareness and seismic resistant measures were introduced at an urban and building level. Extensive and detailed information about the historical condition of the city is available in the literature (Mascarenhas 1996; Correia 1997; Figueiras 1999; SGU 2008; Rossa 2009; Gonçalves 2009), including plans of the original buildings and construction details (also in CAD format). Thus, another seismic vulnerability assessment of VRSA was performed assuming the original building configuration.

As shown in Figure 1, the original urban configuration was extremely homogeneous and was composed of essentially four distinct architectural typologies. The extensive information available allowed performing a detailed seismic vulnerability assessment of each building type. The number of historical buildings evaluated was determined based on the 284 buildings evaluated for the current condition. The space occupied by the current building was compared with the original urban shape to determine the number of buildings to assess. Thus, if, for example, the current building occupies the space of three original single-story dwellings, three buildings of this type were selected for the historical seismic vulnerability assessment. As a result, a total of 403 buildings were considered for the historical condition seismic assessment. This already anticipated that the current buildings are of greater dimensions than the original ones and, thus, prone to be more vulnerable. From these 403 buildings, 8 different building types were identified: (A) single-story dwellings in the corner position of the urban block; (B) single-story dwellings in the mid position of the urban block; (C) the 'towers'; (D) the *alfândega* or Customs House; (E) riverfront buildings; (F) salting factories and warehouses; (G) the square 'towers'; and (H) the square buildings. Table 3 shows the results of the assessment and the number of buildings considered of each type (*N*).

Table 3. Results of the seismic vulnerability assessment on the historical configuration of VRSA

		Historical building type								**Statistics**				
	Units	**A**	**B**	**C**	**D**	**E**	**F**	**G**	**H**					
N	-	75	298	2	1	10	8	3	6	**Mean**	**Minimum**	**Maximum**	**STD**	**CoV**
LS1	*g*	0.38	0.45	0.22	0.19	0.21	0.25	0.28	0.19	0.42	0.19	0.45	0.06	14.60%
LS2	*g*	0.46	0.60	0.37	0.33	0.34	0.30	0.43	0.32	0.56	0.30	0.60	0.08	15.08%
LS3	*G*	0.52	0.68	0.43	0.38	0.39	0.34	0.50	0.37	0.63	0.34	0.68	0.10	15.24%

Given the small scale, good construction quality and regularity of the buildings, the overall vulnerability of VRSA historic city center (assuming the historical configuration) is notably low. Moreover, since the great majority of the building in the historic downtown are single-story dwellings, the final mean values of the load factors defining each LS are much conditioned by the values obtained for type A and B buildings, which represent the 19% and the 74% of the buildings considered, respectively. The mean values of the load factors obtained are significantly higher than the ones obtained for the current condition: 0.42g, 0.56g and 0.63g in the historic condition against 0.15g, 0.35g and 0.42g in the current condition for LS1, LS2 and LS3, respectively. Figure 11 shows the damage scenarios for three different earthquake inputs: (a) $S_e = 0.15g$ $(PGA = 0.11g)$; (b) $S_e = 0.25g$ $(PGA = 0.18g)$; and (c) $S_e = 0.35g$ $(PGA = 0.25g)$, which can be compared with those shown in Figure 9 for the current condition. The maps illustrate the previously commented high seismic resilience of the historical city center, mainly given by the low vulnerability of buildings type A and B, which are the great majority of the historical building stock. Those building typologies are not expected to suffer structural damage for an earthquake of $S_e = 0.35g$ ($PGA = 0.25g$).

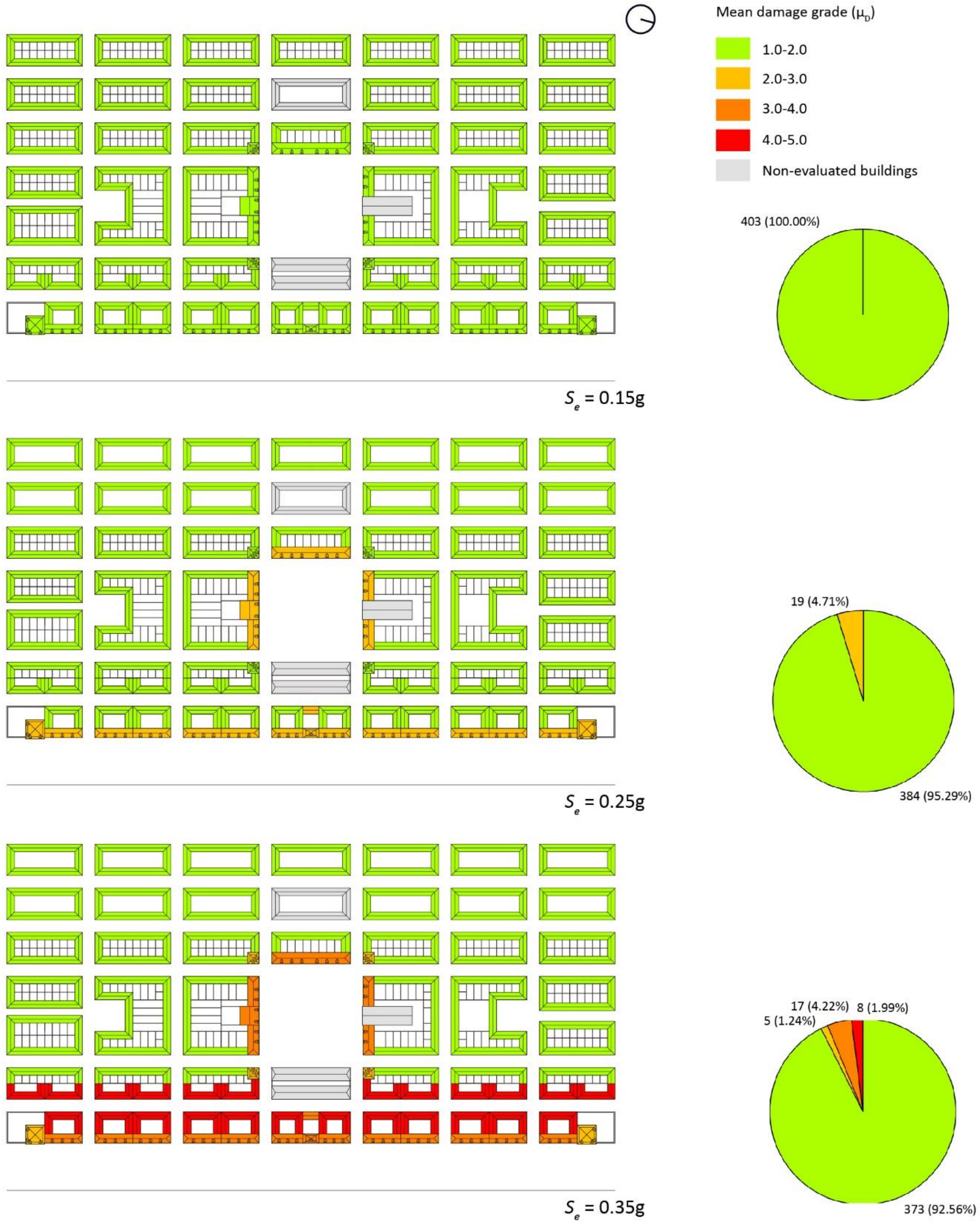

Figure 11. Damage scenarios for different seismic input for the historical condition of VRSA city center, in terms of seismic demand (S_e): (a) 0.15g; (b) 0.25g; and (c) 0.35g

A comparison was also performed in terms of fragility curves, built for the historical condition, using the previously described approaches. A first set of analytical fragility curves is shown in Figure 12a, together with those belonging to the current condition, for comparative purposes. The shift of the curves along the horizontal axis, towards higher values of S_e is an evidence of a notable increase in the seismic vulnerability of VRSA city center, which was very low in the historical condition. For example, for the earthquake defined by the code of $PGA = 0.17g$ $(S_e = 0.24g)$, the percentage of buildings expected to present slight structural damage is extremely low. The second set of empirical fragility curves (Figure 12b) was constructed using Eq. 4 and 5 and also confirms the same trend. The empirical fragility curves show expected drastic changes in the curves, since most of the buildings belong to the same typology. The percentage of buildings ($P[D_k]$) that is expected to exceed each damage grade (D_k) increases drastically after reaching specific values of S_e. The biggest change corresponds to the type B buildings because there are 298 buildings of this type. Figure 12b also shows the comparison between the curves for the historical and the current condition. In the historical condition, only for values of S_e close to 0.4g, there would be buildings that are expected to present severe damage with potential risk of collapse ($\mu_D >$ 4). Nevertheless, for the earthquake defined by the code of $PGA = 0.17g$ $(S_e = 0.24g)$, the great majority of the buildings would be expected to present slight structural damage.

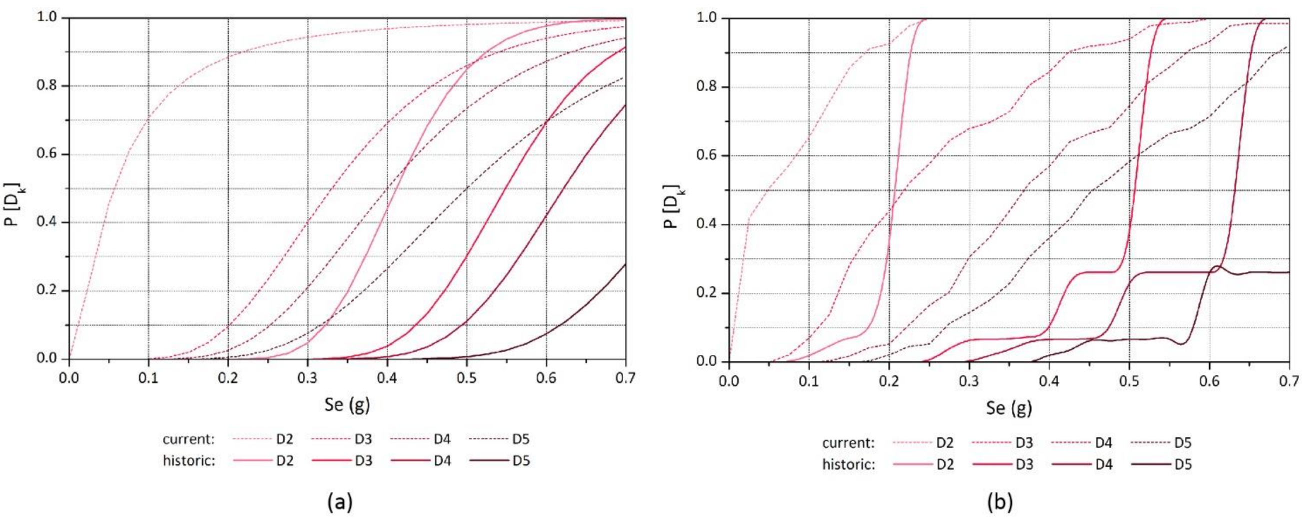

Figure 12. Comparison between the historical and the current condition of the historical building stock of VRSA city center in terms of fragility curves: (a) Analytical; and (b) empirical

This study reflects clearly that the alterations carried out in the building stock have considerably increased the seismic vulnerability of the buildings within VRSA historical city center. It should be also noted that the vulnerability assessment of the current condition has been carried out only for those buildings that still preserve the stone masonry skeleton and the timber diaphragms. Most buildings in VRSA city center show further level of intervention with poorly planned additions, new materials, alterations of the structural type, additions of parts structurally incompatible with the existing ones, etc. The increase in the overall seismic vulnerability in the city center can be even higher.

4.4. Seismic vulnerability mitigation

The last scenarios that are studied herein result from the application of different building retrofitting strategies based on traditional earthquake resistant solutions. This study is meant to serve as: (a) an example of the usefulness of seismic vulnerability assessment methods in the decision-making process involved in risk management and mitigation, and its capability as a general planning tool; and (b) putting the focus on using traditional strengthening techniques to preserve our historical built-up environments. These solutions were developed empirically by local communities to protect their built-up environment and have become traditional because they have continually proven to be effective in resisting past seismic events (Ortega et al. 2017). Recent research has focused on evaluate quantitatively their actual efficiency through experimental (Murano 2018) and numerical work (Ortega et al. 2018). Gaining confidence on the use of these techniques is not only good in terms of compatibility and authenticity (satisfying the current principles of preservation), but can also help preventing the abandonment of vernacular buildings that are many times considered unsafe. VRSA is an example of how the loss of knowledge on traditional materials and construction techniques generally leads to the demolition and reconstruction of buildings using modern materials, with the consequent invaluable loss of heritage while not improving their seismic safety.

The selection of the retrofitting strategies was done following three main steps: (1) selection of the most vulnerable buildings in which to implement the selected techniques according to the LS3 distribution shown in Figure 7; (2) identification of the parameters showing the worst classification according to the parameter class distribution of the evaluated buildings (Table 2); and (3) selection of the most appropriate techniques that can be used to upgrade the seismic vulnerability classes of the previously identified parameters, according to those previous numerical studies on the assessment of their efficiency, see Ortega et al. (2018).

A total of 33 buildings were selected based on the values of load factor associated to LS3 below 0.25g, which is close to the seismic demand computed with Eq. 1 from the PGA established by the code of 0.17g (NP EN1998-1 2010). A common characteristic of the 33 buildings that show higher vulnerability is that they have greater dimensions than the typical buildings from VRSA city center. Most of them have two or more floors and/or have long facades walls presumably spanning large distances (high values for P2). It should be noted that, prior to the definition of a retrofitting strategy, a more detailed assessment is always recommended, in order to confirm the real condition of the building. For instance, regarding P2, the interior configuration should be evaluated in detail to confirm that there are not intermediate supports well connected to the façade wall that can be considered as shear walls. Figure 13 shows examples of some of the buildings showing higher vulnerability.

Figure 13. Examples of the 33 buildings in VRSA selected for the application of retrofitting solutions

Another common characteristic of the selected buildings is the use of timber horizontal diaphragms that provide poor or no proper connection among the resisting walls (class 4 for P5). The lack of proper connection between the roofs and the walls also results in assuming that the pitched roof types observed are exerting thrust on the walls (class 2 or 3 for P6). Finally, most of these buildings also present previous structural damage and significant cracks in the walls due to a poor state of conservation and even abandonment in some cases (class 2 or 3 for P9).

Taking the above into account, a first retrofitting strategy (A) could consist of directly addressing the horizontal diaphragms and improving their connection to the walls. A common solution would consist of reinforcing the floor-to-wall and roof-to-wall connections and stiffening floors and roofs. A proper intervention of this type could result in upgrading the class of P5 to 2 in all directions. The reinforced roof-to-wall connection would also result in an upgrade of P6 class to 1, since they would prevent the roof thrust. This retrofitting strategy and the followings should always include repairing the existing cracks and a proper conservation intervention of the structural elements in order to upgrade P9 class to 1.

A second retrofitting strategy (B), more invasive towards the urban public space, but traditionally applied in historical centers, could consist of the construction of buttresses or urban reinforcing arches within the span of the wall. This strategy would aim at minimizing the façade free span (reducing the values for P2). This solution has also an impact on the urban design and thus it might not be the most appropriate also in terms of the preservation of heritage values of VRSA. It might be more adequate for other contexts, such as rural environments, with not such a strong urban design value. It should be thus noted that this study is mainly intended to show the capabilities of this procedure to decide on vulnerability mitigation decisions at an urban level, which should always be taken among all the different agents involved in the process. Finally, the third strategy (C) proposed would be the application of the previous two techniques plus the addition of timber ring beams at the roof and floor levels of the buildings. This technique will upgrade the class of P5 to 1. However, it is noted that the implementation of this last strategy is more complex and costlier in terms of construction. At the level of the roof, it might require the raising and removal of the roof. At the floor level, their installation is challenging, since it may require the removing or cut of some masonry courses or the drilling through the wall thickness, as it can be observed in previous examples of the application of ring beams to retrofit existing earthen and masonry buildings (Magenes et al. 2014; Lourenço et al. 2019).

Table 4 shows the changes in the results using both methods. All retrofitting strategies have a clear impact on the overall vulnerability of the historical VRSA city center. Since the intervention is only considered for 33 buildings (12% of the total evaluated buildings), the changes in the mean values are not so evident. However, there is a significant difference concerning the minimum and maximum values. The minimum value of LS3 is basically doubled from 0.13g to 0.25g using strategy A. Also, the retrofitted buildings using strategy C reach high values of LS3, exhibiting a high seismic resistance. The mean value of LS3 assuming this scenario increases from 0.42g to 0.49g, which is also a significant difference.

The differences are also visible in terms of fragility curves (Figure 14). Note that both the analytical and the empirical sets of fragility curves were prepared and shown in Figure 14a and b, respectively. The trend observed in both sets is similar. There is a notable reduction of the number of buildings ($P[D_k]$) that are expected to exceed each damage grade, particularly for values of $S_e < 0.25g$. The three retrofitting strategies are efficient in delaying the occurrence of severe damage with potential risk of collapse ($\mu_D > 4$). Strategy C is the most effective but also the costliest because requires a greater intervention. Strategy A, on the contrary, only intervenes at the diaphragm level, and proves to effectively reduce the seismic risk. For instance, for the earthquake used as reference from the code of $S_e = 0.24g$ $(PGA = 0.17g)$, this primary safety assessment shows that less than 5% of the buildings is expected to show severe damage and risk of collapse ($\mu_D > 4$). It should be highlighted the results of first level simplified assessments should be taken as a first estimation and interpreted in comparative terms. The process followed to define the retrofitting scenarios is nevertheless a valuable tool to define other scenarios in order to assess the efficiency of different traditional strengthening solutions and their overall effect on the building stock. Also, in order to further reduce the seismic vulnerability of VRSA historical city center, the number of buildings intervened can be enlarged up to a satisfactory result.

Table 4. Results of the seismic vulnerability assessment on the different retrofitted scenarios assumed for VRSA

Retrofitting strategy		$\overline{LS}$	**Min**	**Max**	**STD**	**CoV (%)**
Current	LS1 (g)	0.15	0.00	0.50	0.14	93.21
	LS2 (g)	0.35	0.10	0.69	0.13	35.88
	LS3 (g)	0.42	0.13	0.79	0.14	33.03
A	LS1 (g)	0.16	0.00	0.50	0.13	78.99
	LS2 (g)	0.38	0.20	0.69	0.11	29.76
	LS3 (g)	0.45	0.25	0.79	0.12	27.19
B	LS1 (g)	0.16	0.00	0.50	0.13	83.67
	LS2 (g)	0.37	0.15	0.69	0.11	30.58
	LS3 (g)	0.44	0.18	0.79	0.12	28.10
C	LS1 (g)	0.18	0.00	0.81	0.16	87.53
	LS2 (g)	0.41	0.20	1.08	0.16	37.68
	LS3 (g)	0.49	0.26	1.23	0.17	34.76

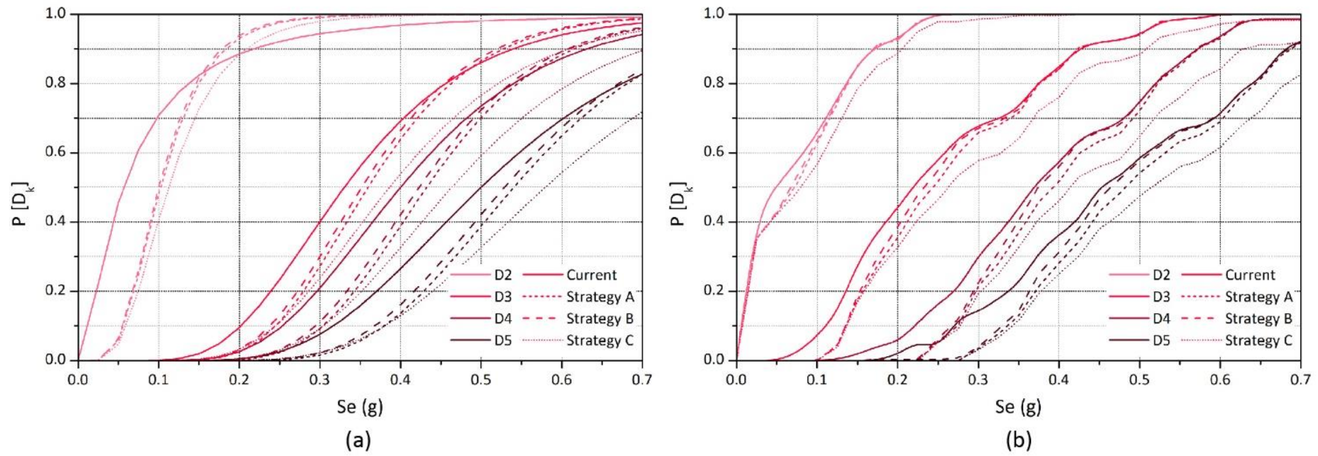

Figure 14. Comparison between the four different scenarios considered in terms of fragility curves: (a) analytical fragility curves; (b) empirical fragility curves

The results obtained can also be presented using the GIS tool, showing the damage scenarios for an earthquake with $S_e = 0.25g$ $(PGA = 0.18g)$ considering the three different retrofitting strategies, see Figure 15. They can be compared with the same scenario for the current condition shown in Figure 9 in order to see how the collapse of several buildings is avoided. For example, no buildings are expected to suffer collapse considering the retrofitting strategies A and C.

Figure 15. Damage scenarios for an earthquake with $S_e = 0.25g$ $(PGA = 0.18g)$ considering the three retrofitting strategies

5. Seismic loss assessment

Finally, the loss assessment for the buildings was evaluated for the historical city center of VRSA. Results are also presented using the GIS tool to visualize the loss scenarios. The losses are estimated as a function of the probability of exceedance of certain damage grades using methodologies available in the literature and previously applied in similar seismic vulnerability assessments. It is noted that the discussion of the expressions applied for the loss assessment is out of the scope of this work. The loss estimation obtained for the current condition is also contrasted with the historical and retrofitted condition, in order to better understand: (a) the effects of the alterations undergone by VRSA city center in terms of losses; and (b) the impact of the retrofitting strategies in the reduction of human and economic losses.

5.1. Collapsed and unusable buildings

The loss estimation models used for assessing the probability of building collapse and loss of functionality are based on the work developed by Bramerini et al. (1995) after post-earthquake damage observation. The probability is thus calculated by using multiplier factors ranging from 0 to 1 on the probability (p_k) associated to certain damage grades D_k ($k \in [0,5]$):

$$P_{collapse} = p_5 \tag{6}$$

$$P_{unusable} = 0.4 \times p_3 + 0.6 \times p_4 \tag{7}$$

The factors 0.4 and 0.6 are adopted from Vicente et al. (2011). Figure 16 shows the results for the current condition of VRSA, mapped using the GIS tool and considering a seismic event with $S_e = 0.25g$ ($PGA = 0.18g$). Overall results for different seismic events with increasing S_e and for the three different scenarios are summarized in Table 5, where it is worth highlighting the low vulnerability of the historical condition, particularly in comparison with the current configuration. Finally, Figure 17a depicts the probability of collapsed and unusable buildings based on the percentage of buildings that are expected to exceed each damage grade shown in Figure 10b, i.e. according to the empirical fragility curves. Figure 17b shows the comparison between the current, historic and retrofitted scenario (considering the application of strategy A).

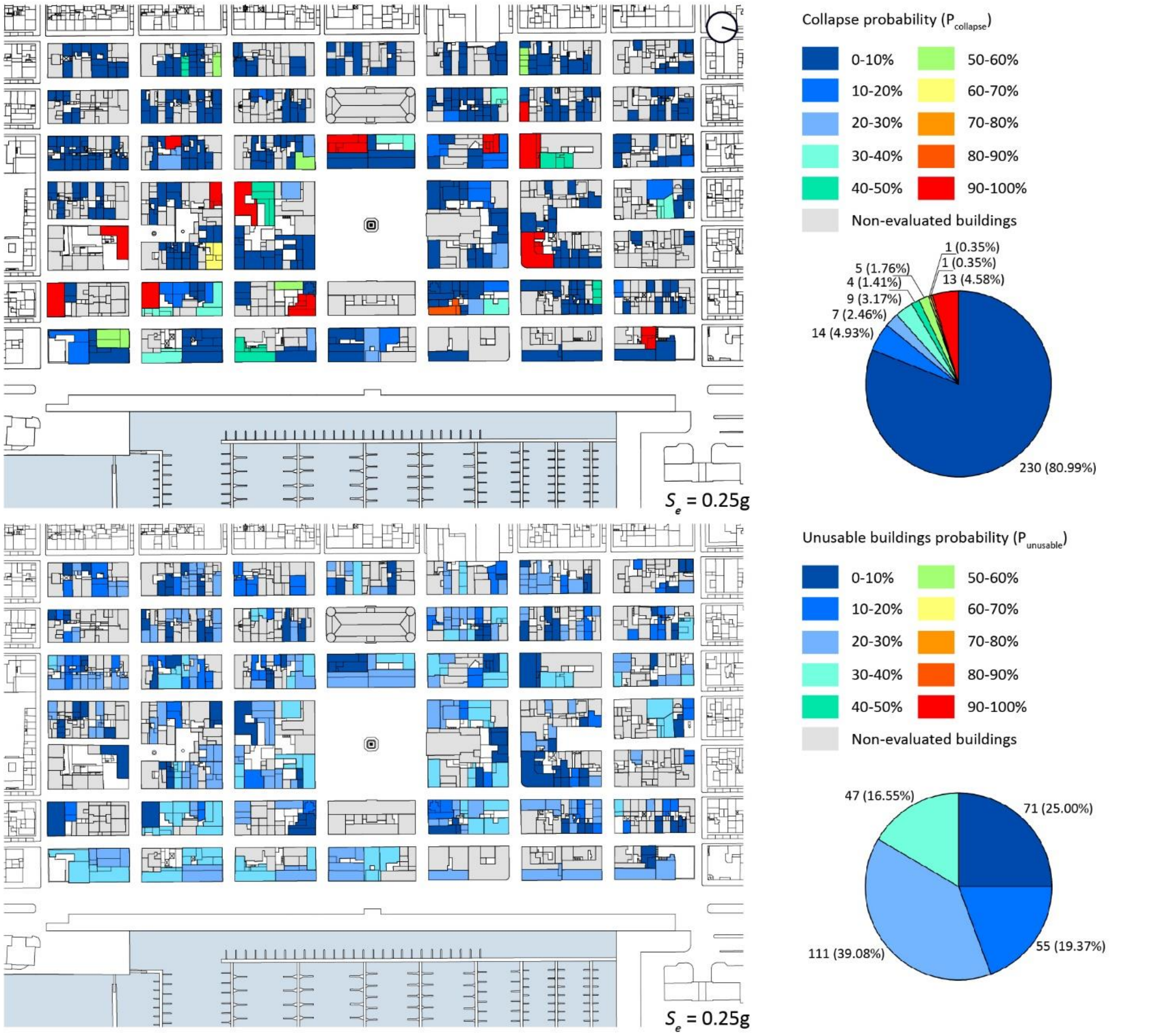

Figure 16. Collapsed and unusable buildings loss scenarios in the current condition: $S_e = 0.25g$ $(PGA = 0.25g)$

Table 5. Number of collapsed and unusable buildings for the three different scenarios considered

N = 284	**Current condition**				**Historical condition**				**Retrofitted condition**			
	S_e (g)				S_e (g)				S_e (g)			
	0.15	0.25	0.35	0.45	0.15	0.25	0.35	0.45	0.15	0.25	0.35	0.45
Collapsed	0	15	65	140	0	0	0	6	0	0	37	122
Unusable	33	66	69	58	0	0	10	23	19	60	79	67

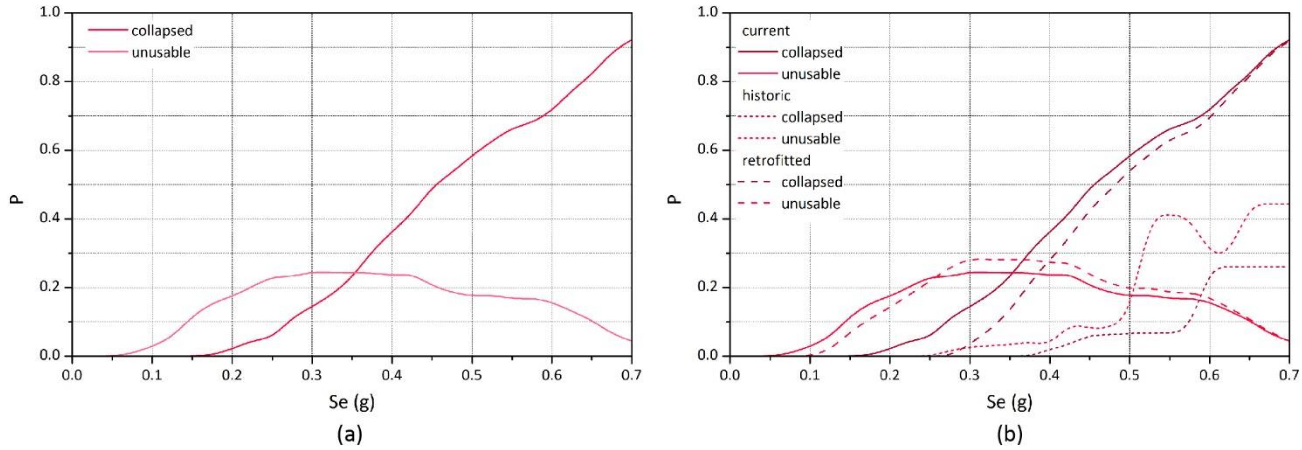

Figure 17. (a) Probability of collapsed and unusable buildings in the current condition; and (b) comparison with the historic and retrofitted condition (strategy A)

5.2. Human casualties and homelessness

The work developed by Bramerini et al. (1995) served also as a basis for the loss estimation models used for assessing the casualty rates (deaths and severely injured) and homelessness. The multiplier factors adopted were also adopted from Vicente et al. (2011). The casualty rates are considered as being 30% of the residents of collapsed buildings (Eq. 8). The amount of homeless people that will require shelter after the event is estimated using Eq. 9:

$$\mathrm{P}_{dead\ and\ severely\ injured} = 0.3 \times \mathrm{p}_5 \tag{8}$$

$$\mathrm{P}_{homeless} = 0.4 \times \mathrm{p}_3 + 0.6 \times \mathrm{p}_4 + 0.7 \times \mathrm{p}_5 \tag{9}$$

Figure 18 shows these results mapped using the GIS tool and considering a seismic event with an expected $S_e = 0.25g$ $(PGA = 0.18g)$. Overall results for different seismic events with increasing S_e and for the three different scenarios are summarized in Table 6. The total number of inhabitants living in the 284 buildings evaluated was considered as 1784. The reduction of the number of casualties for the retrofitted scenario is significant, particularly for a seismic event of $S_e = 0.25g$ $(PGA = 0.18g)$, where the number of dead or severed injured is reduced from 28 to 0. Finally, Figure 19a depicts the estimation of the number of casualty rates and homeless based again on the percentage of buildings that are expected to exceed each damage grade according to the empirical fragility curves (Figure 10b). Figure 19b shows the comparison with the historic and the retrofitted scenario A.

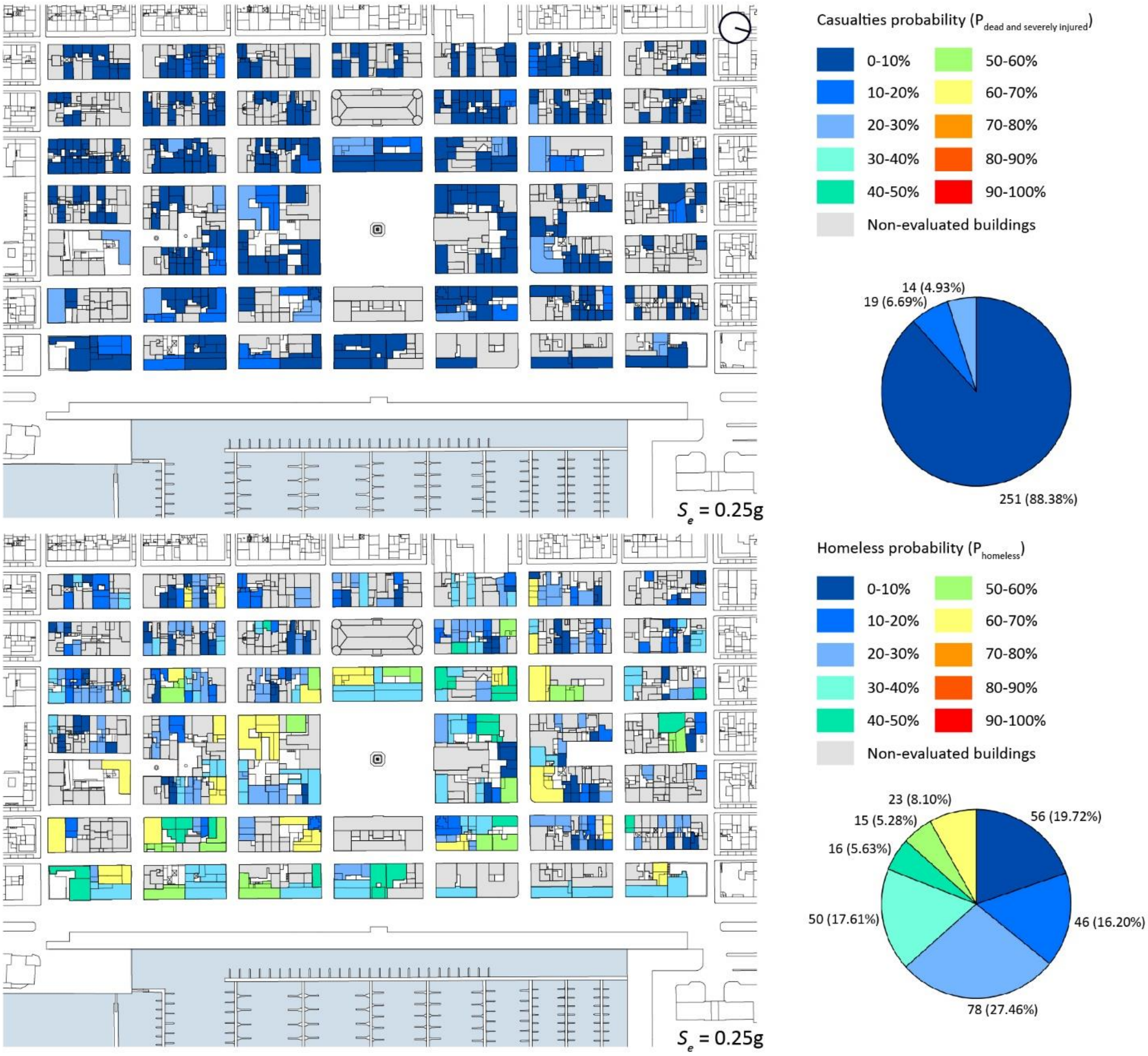

Figure 18. Casualties and homeless estimation scenarios in the current condition: $S_e = 0.25g$ $(PGA = 0.25g)$

Table 6. Number of dead or severely injured and homeless people for the three scenarios considered

N = 1784	**Current condition**				**Historical condition**				**Retrofitted condition**			
	S_e (g)				S_e (g)				S_e (g)			
	0.15	0.25	0.35	0.45	0.15	0.25	0.35	0.45	0.15	0.25	0.35	0.45
Dead or severely injured	0	28	122	264	0	0	0	5	0	0	70	230
Homeless	207	481	718	981	0	0	10	35	121	379	660	959

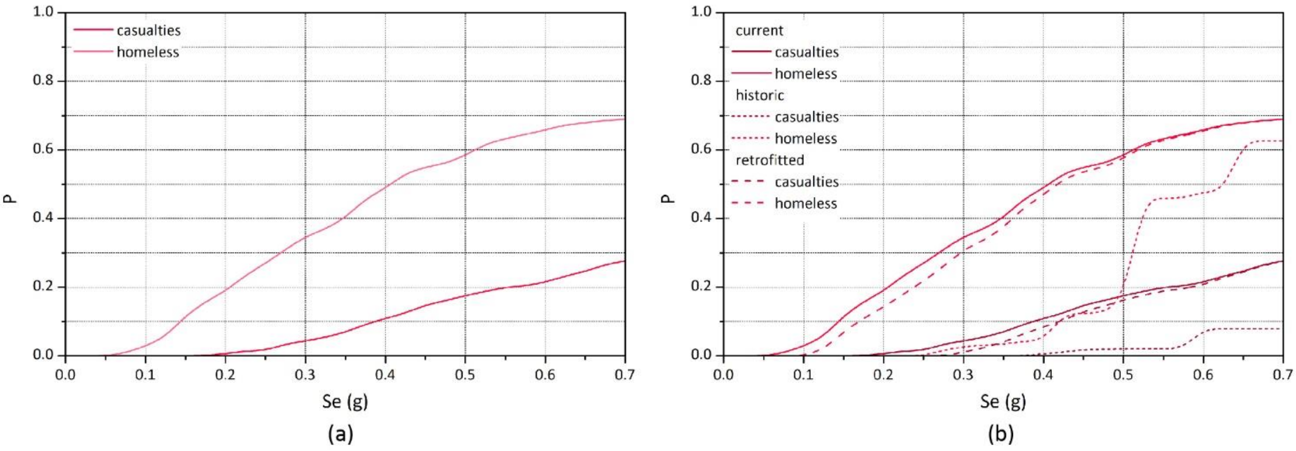

Figure 19. (a) Probability of casualties and homeless in the current condition; and (b) comparison with the historic and retrofitted condition (strategy A)

5.3. Economic loss and repair cost estimation

The economic loss estimation models used in the present study are based on establishing a correlation between the damage grades (D_k) and the estimated repair and rebuilding costs, expressed in terms of an economic damage index, following the approach suggested by Vicente et al. (2011). The economic damage index can be defined as the ratio between the repair cost and the replacement cost of the building. Several correlations between damage grades and economic damage index exist in the literature and are typically established after post-seismic investigation. The one applied in this study was established by Dolce et al. (2006), calibrated after the Umbria Marche (1997) and Pollino (1998) earthquakes. The correlation between damage grades and damage economical index is shown in Table 7.

Table 7. Correlation between damage grades D_k and damage index

Damage grade (D_k)	**0**	**1**	**2**	**3**	**4**	**5**
***P[R|D_k]* (Dolce et al. 2006)**	0.005	0.035	0.145	0.305	0.800	0.950

The probability of repair costs (expressed in terms of the economic index ranging from 0 to 1) that would be required after an earthquake (P_{repair}) can be estimated by multiplying the conditional probability of the repair costs for each damage level ($P[R|D_k]$), using the values shown in Table 7, with the probability (p_k) associated to the different damage grades:

$$\mathrm{P}_{repair} = \sum_{k=1}^{5} \mathrm{P}[\mathrm{R}|D_k] \times p_k \quad (10)$$

It is noted that damage grade 0 is not included because the SAVVAS method considers that damage grades 0 and 1 are the same, since it does not detect non-structural damage. The estimated cost of repairing the building stock of VRSA city center was calculated by considering an average cost value of 800 €/m^2 as the replacement cost of the buildings. The resulting estimated repairing cost can be expressed as a function of the seismic input in terms of seismic demand (S_e), see Figure 20a. The figure also includes the costs estimated for the retrofitted scenario A, which shows that the difference in the repair costs can be significant by making a preventive intervention in 33 buildings and can reach up to 2.5 million of euros for a seismic event with $S_e = 0.25g$ $(PGA = 0.18g)$.

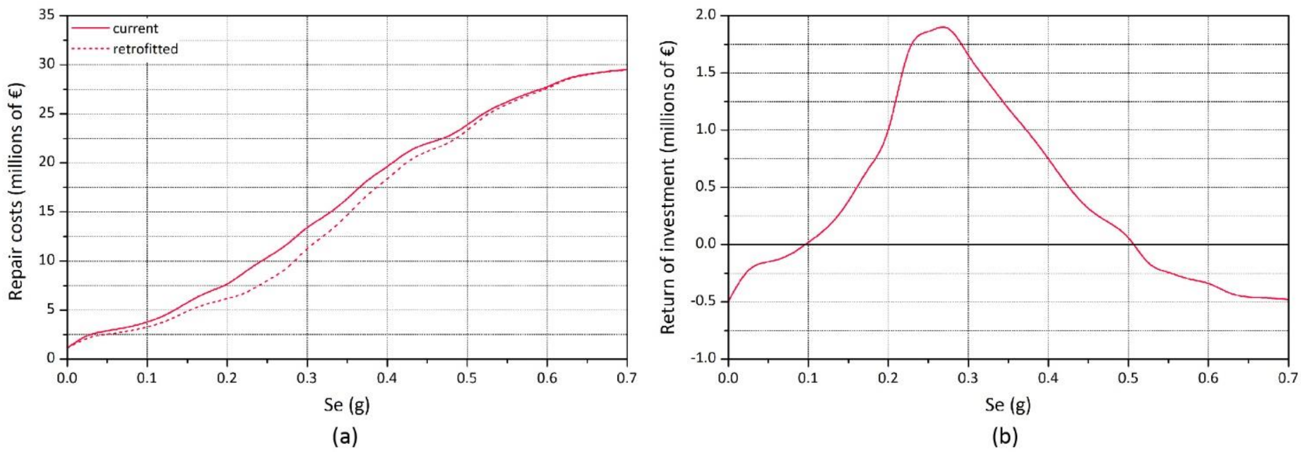

Figure 20. (a) Estimation of repair costs for the current and retrofitted condition (strategy A); and (b) return of the investment of the retrofitting strategy A as a function of the seismic event in terms of seismic demand (S_e)

Figure 20b presents the return of the investment of the retrofitting strategy A as a function of S_e. Diz et al. (2015) estimated the cost of the retrofitting solution included in strategy A, consisting of strengthening the diaphragm-to-wall connections, at 23€/m^2. This value was increased up to 50€/m^2 considering additional costs associated to the intervention, such as the stiffening of the diaphragms and the repairing of cracks. This value is in line with other values shown in the literature based on strengthening works carried out in Azores after 1998 earthquake (Costa et al. 2013). The graph shows that the initial costs of the intervention are promptly compensated economically. This fact, together with the reduced loss in terms of collapse buildings and human casualties shown in Table 5 and Table 6, justifies the need of preventive action regarding seismic protection including the retrofitting of the existing building stock. It should be noted that this simplified cost-benefit analysis is primarily aimed at showing the potentialities of using this tool for making decisions regarding risk management and control. A deeper study of the implementation costs of the different traditional solutions to perform a more robust cost-benefit analysis is out of the scope of this work. Finally, overall results for different seismic events with increasing PGA and for the current and retrofitted scenarios are summarized in Table 8.

Table 8. Estimation of the repair costs for the current and retrofitted scenarios considered

N = 284	**Current condition**				**Retrofitted condition**			
	S_e (g)				S_e (g)			
	0.15	0.25	0.35	0.45	0.15	0.25	0.35	0.45
Repair costs (in millions of €)	5.8	10.37	16.28	22.04	4.94	8.03	14.60	21.24

6. Conclusions

The present paper presented the application of the novel Seismic Assessment of the Vulnerability of Vernacular Architecture Structures (SAVVAS) method at the historical city center of Vila Real de Santo António, in the South of Portugal. It has shown the applicability of the method to large scale analysis. The use of a GIS tool allowed the storage of the results associated to the urban plan of the city. Thus, results could be presented in different maps, allowing an easy visualization and the quick detection of the most vulnerable buildings. The most significant uncertainty of the method, as with methods from the literature, is related to the input information and the inspection phase. Since not all the buildings could be inspected in detail, not all the data required to complete the parameter survey is completely reliable. However, the available information included sufficiently detailed reports and photographs of enough buildings to be confident on the results obtained. Even though a general low level of damage was estimated for the buildings of VRSA, a significant amount of buildings showing a worrisome vulnerability were identified and recommended for a more detailed assessment.

Two additional scenarios were considered for the seismic vulnerability assessment. Firstly, the vulnerability of the historical condition of the city at the moment of its construction was evaluated, since detailed information was available. The objective was to understand if the structural alterations undergone by the buildings in VRSA city center have resulted in an increase of the seismic vulnerability, and to measure this increment. There has been a notable increase of the vulnerability with respect to the historical configuration, whose resistance to seismic actions is very high. Secondly, several retrofitting strategies were defined based on traditional strengthening techniques and applied to a total of 33 buildings of VRSA, which were identified as the most vulnerable to seismic actions. The reduction of the overall vulnerability of the city center was then evaluated and proved to be efficient in reducing the number of buildings that are expected to exceed the different damage levels defined, particularly for earthquakes with values of seismic demand (S_e) lower than 0.25g.

In the end, the paper presented the seismic loss assessment for the city center of VRSA, including the estimation of the amount of collapsed and unusable buildings, number of casualties and homelessness, and the economic loss and repair costs. The losses were also estimated for the historic and retrofitted condition in order to further investigate the differences among the three scenarios. Particularly with respect to the retrofitted scenario, results show that investing in retrofitting using traditional strengthening solutions would result in economic benefits in the event of an earthquake. More importantly, it would also provide a significant reduction of the number of collapsed buildings and possible human casualties. In summary, the paper provides a deep insight of the capabilities of large-scale seismic vulnerability assessment in managing seismic risk and making decisions on rehabilitation strategies of old urban areas. In particular, it validates the applicability of the novel SAVVAS method for this matter.

Acknowledgments

The work presented in this paper was partly financed by FEDER funds through the Competitivity and Internationalization Operational Programme – COMPETE and by national funds through FCT – Foundation for Science and Technology within the scope of the project POC1-01-01-0145-FEDER-007633.

References

Benedetti D, Petrini V (1984) Sulla Vulnerabilità Di Edifici in Muratura: Proposta Di Un Metodo Di Valutazione, L'industria delle Costruzioni 149 (1): 66-74

Boukri M, Bensaibi M (2008) Vulnerability Index of Algiers Masonry Buildings, in: Proc. of 14th World Conference on Earthquake Engineering, Beijing, China

Bramerini F, Di Pasquale G, Orsini A, Pugliese A, Romeo R, Sabetta F (1995) Rischio sismico del territorio italiano. Proposta per una metodologia e risultati preliminary, Rapporto tecnico del Servizio Sismico Nazionale (SSN), Roma, Italy

CEN (2004) Eurocode 8: Design of structures for earthquake resistance – part 1: General rules, seismic actions and rules for buildings, European Committee for Standardization (CEN), Brussels, Belgium

Correia J (1997) Vila Real de Santo António. Urbanismo e Poder na Política Pombalina, Ph.D. thesis, Faculdade de Arquitectura da Universidade de Porto, Portugal

Costa AA, Arêde A, Campos Costa A, Penna A, Costa A (2013) Out-of-plane behaviour of a full scale stone masonry façade. Part 1: specimen and ground motion selection, Earthquake Engineering and Structural Dynamics 42: 2081-2095

Diz S, Costa A, Costa AA (2015) Efficiency of strengthening techniques assessed for existing masonry buildings, Engineering Structures 101: 205-215

Dolce M, Kappos A, Masi A, Penelis G, Vona M (2006) Vulnerability assessment and earthquake damage scenarios of the building stock of Potenza (southern Italy) using Italian and Greek methodologies, Engineering Structures 28 (3): 357-371

Esri (2017) Environmental Systems Research Institute (ESRI), Inc.

FEMA (2010) HAZUS-MH MR4: Technical Manual, Vol. Earthquake Model, Federal Emergency Management Agency, Washington DC, US

Ferreira TM, Vicente R, Varum H (2014) Seismic vulnerability assessment of masonry facade walls: development, application and validation of a new scoring method, Structural Engineering and Mechanics 50 (4): 541-561

Ferreira TM, Maio R, Vicente R (2017) Seismic vulnerability assessment of the old city centre of Horta, Azores: calibration and application of a seismic vulnerability index method, Bulletin of Earthquake Engineering 15 (7): 2879-2899

Giovinazzi S, Lagomarsino S (2004) A macroseismic model for the vulnerability assessment of buildings, in Proc. of 13th World Conference on Earthquake Engineering, Vancouver BC, Canada

Gonçalves A (2005) Caracterização do Núcleo Pombalino, ECDJ 9: 18-35, Universidade de Coimbra, Portugal

Gonçalves A (2009) Vila Real de Santo António. Planeamento de pormenor e salvaguarda em desenvolvimento, Monumentos (30): 40-53

Grünthal G (1998) European Macroseismic Scale 1998 (EMS-98), European Seismological Commission, Subcommission on Engineering Seismology. Working Group Macroseismic Scales, Cahiers du Centre Européen de Géodynamique et de Séismologie 15

Lourenço PB, Ciocci MP, Greco F, Karanikoloudis G, Cancino C, Torrealva D, Wong K (2019) Traditional techniques for the rehabilitation and protection of historic earthen structures: The seismic retrofitting project, International Journal of Architectural Heritage 13(1): 15-32

Magenes G, Penna A, Senaldi IE, Rota M, Galasco A (2014) Shaking Table Test of a Strengthened Full-Scale Stone Masonry Building with Flexible Diaphragms, International Journal of Architectural Heritage 8: 349-375

Mascarenhas JMD (1996) A study of the design and construction of buildings in the Pombaline quarter, Ph.D. thesis, University of Glamorgan, UK

Murano A (2018) Out-of-plane behaviour of stone masonry walls built with earthquake resistant techniques, M.Sc. thesis, University of Minho, Portugal

NP EN1998-1 (2010) Eurocódigo 8 – Projecto de estruturas para resistência aos sismos–Parte 1: Regras gerais, acções sísmicas e regras para edifícios (Anexo Nacional), CEN

Ministerio delle Infrastrutture e dei Transporti (MIT) (2018) Circolare aplicativa delle nuove norme tecniche per le costruzioni approvate com D.M. 17 gennaio 2018, Consiglio Superiore dei Lavori Pubblici n. 29/2017, Servizio Tecnico Centrale

Ministerio delle Infrastrutture e dei Transporti (MIT) (2018) Norme tecniche per le costruzioni, Decreto 17 gennaio 2018, Consiglio Superiore dei Lavori Pubblici, Servizio Tecnico Centrale

Oliveira A (2009) Casa da Câmara de Vila Real de Santo António. Levantamento arqueológico, Monumentos (30): 54-61

Ortega J, Vasconcelos G, Rodrigues H, Correia M (2016) Seismic behavior of an old masonry building in Vila Real de Santo António, Portugal, in: Proc. of the 10th International Conference on Structural Analysis of Historical Constructions, SAHC 2016, Leuven, Belgium

Ortega J, Vasconcelos G, Rodrigues H, Correia M, Lourenço PB (2017) Traditional earthquake resistant techniques for vernacular architecture and local seismic cultures: A literature review, Journal of Cultural Heritage 27: 181-196

Ortega J, Vasconcelos G, Rodrigues H, Correia M (2018) Assessment of the efficiency of traditional earthquake resistant techniques for vernacular architecture, Engineering Structures 173

Ortega J (2018) Reduction of the seismic vulnerability of vernacular architecture with traditional strengthening solutions, Ph.D. thesis, University of Minho, Guimarães, Portugal

Ortega J, Vasconcelos G, Rodrigues H, Correia M, Miranda T (2019a) Development of a Numerical Tool for the Seismic Vulnerability Assessment of Vernacular Architecture, Journal of Earthquake Engineering

Ortega J, Vasconcelos G, Rodrigues H, Correia M, Ferreira TM, Vicente R (2019b) Use of post-earthquake damage data to calibrate, validate and compare two seismic vulnerability assessment methods for vernacular architecture, International Journal of Disaster Risk Reduction 39

Rossa W (2009) Cidades da razão: Vila Real de Santo António e arredores, Monumentos (30): 16-31

Saloustros S, Pelà L, Contrafatto FR, Roca P, Petromichelakis I (2019) Analytical Derivation of Seismic Fragility Curves for Historical Masonry Structures Based on Stochastic Analysis of Uncertain Material Parameters, International Journal of Architectural Heritage 13(7): 1142-1164

Shakya M (2014) Seismic vulnerability assessment of slender masonry structures, Ph.D. thesis, Universidade de Aveiro, Aveiro, Portugal

SGU (2008) Plano de Pormenor de Salvaguarda do Núcleo Pombalino de Vila Real de Santo António, Sociedade de Gestão Urbana (SGU) de Vila Real de Santo António

Vicente R, Parodi S, Lagomarsino S, Varum H, Mendes da Silva JAR (2011) Seismic vulnerability and risk assessment: a case study of the historic city centre of Coimbra, Portugal, Bulletin of Earthquake Engineering 9 (4): 1067-1096